Annual Review of Condensed Matter Physics

The Fokker–Planck Approach to Complex Spatiotemporal Disordered Systems

J. Peinke,[1,2] M.R.R. Tabar,[3] and M. Wächter[1]

[1]Institute of Physics and ForWind, University of Oldenburg, Oldenburg, D-26111, Germany; email: joachim.peinke@uni-oldenburg.de

[2]Fraunhofer Institute for Wind Energy Systems, D-26129 Oldenburg, Germany

[3]Department of the Physics, Sharif University of Technology, Theran, Iran 1397

Annu. Rev. Condens. Matter Phys. 2019. 10:107–32

The *Annual Review of Condensed Matter Physics* is online at conmatphys.annualreviews.org

https://doi.org/10.1146/annurev-conmatphys-033117-054252

Keywords

multipoint statistics, stochastic process, Fokker–Planck equation, self-similarity, short time forecast, nonequilibrium thermodynamics, integral fluctuation theorem

Abstract

When the complete understanding of a complex system is not available, as, e.g., for systems considered in the real world, we need a top-down approach to complexity. In this approach, one may desire to understand general multipoint statistics. Here, such a general approach is presented and discussed based on examples from turbulence and sea waves. Our main idea is based on the cascade picture of turbulence, entangling fluctuations from large to small scales. Inspired by this cascade picture, we express the general multipoint statistics by the statistics of scale-dependent fluctuations of variables and relate it to a scale-dependent process, which finally is a stochastic cascade process. We show how to extract from empirical data a Fokker–Planck equation for this cascade process, which allows the generation of surrogate data to forecast extreme events as well as to develop a nonequilibrium thermodynamics for the complex systems. For each cascade event, an entropy production can be determined. These entropies accurately fulfill a rigorous law, namely the integral fluctuations theorem.

1. INTRODUCTION

For quite some time, research on complex systems has been considered a continuation of investigating nonlinear or chaotic dynamics. The main difference between these systems may be understood by realizing that nonlinear or chaotic systems are spatially homogeneous and, thus, are described by low-dimensional nonlinear differential equations (cf. 1, 2), whereas complex systems possess spatial and temporal inhomogeneities. Due to the interdependence, relationships, or interactions between units of a complex system, the understanding of the entire system is not attainable simply by understanding each part or by understanding the local features. Complex systems are in general composed of many interacting subunits, in which nonlinearities play an important role, so that complex spatiotemporal structures emerge (see, e.g., References 3 and 4). A consequence of the interaction between the subsystems and the overall behavior is that it is often difficult to achieve full comprehensive understanding of complex systems dynamics. Additionally, surprising new collective phenomena may emerge. Examples of emergent behaviors include short- and long-term climate changes, hurricanes, cascading failures, evolution, learning, and intelligence, to name just a few (5).

In this review, we take turbulent flows and sea waves as examples of complex systems. The main task for a good understanding of the appealing complexity of flow patterns, like that shown in **Figure 1**, is to characterize the clearly visible structures (see the sidebar titled Structures), as well

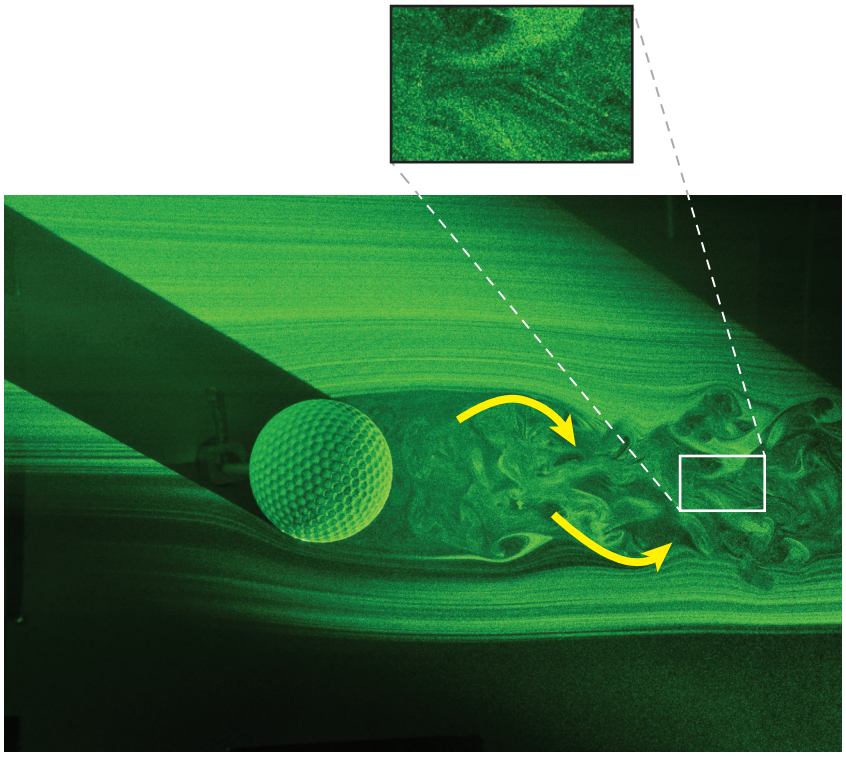

Figure 1

Smoke visualization of flow patterns of a turbulent wake behind a sphere with dimples. The overall structure of the wake flow is recognized right away by its large structures, highlighted by arrows. A closer look at this turbulent wake shows that flow patterns are never repeated exactly either in time or space (see *inset*). For many complex disordered systems, the challenge is to understand this interplay between clear structures and stochasticity.

STRUCTURES

Because the term structures is used throughout this paper, we identify some basic features of structures. Although the word structures is often used in the discussion of complex systems, it remains a rather imprecise term (7). As pointed out by Hussain (13), the scientific treatment of structures is based on visualization; thus, a subjective visual cognition naturally comes into play (see the discussion of **Figure 1**). Structures denotes somehow orderly components of the complex system. The denotation quasideterministic structures expresses the aim to achieve a mathematical description. Particularly for fluid dynamics and turbulence, the term coherent structure is often used, which is defined as "spatially phase correlated velocities or vorticities over the extent of a structure" in Reference 13. This phase correlation allows determination of the form of structures by an averaging method, which becomes complicated if such structures are not fixed to a specific location or time and if they have different sizes. For fluid dynamics, coherent structures are often linked to vorticity structures, like vortex filaments in a boundary layer stretched to the hairpins.

In the following, we sum up several features and definitions of structures used in the context of complex systems. We list these features side by side without claiming any completeness and without asking that all features be valid at the same time.

- Structures have orderly components, persist in form, and have typical length scale.
- Structures are based on a clear mathematical description of a form in real or Fourier space.
- Structures allow a system to be broken down into structures and some incoherent or noise background.
- Structures are linked to special features of the system, like mass, momentum, or energy transport.

In the context of this review, we should note that structures in complex systems often have higher-dimensional forms, like a vortex tube in fluid dynamics. In our contribution, on one hand, we limit the discussion to one-dimensional cuts, which may fade out clear structures and which cannot encompass eddies or vortex-like structures in the case of turbulence. On the other hand, multipoint statistics is used, which enables understanding coherences with respect to higher-order statistics. In Section 7, we consider structures that are linked to entropy values, particularly those that are marked by the consumption of entropy (negative entropy events). Based on a thermodynamical interpretation, a higher order can be attributed to these entropy-consuming events. But finally, we show by the statistics of the entropy values and its rigorous fluctuation law that such entropy structures must be taken as a part of the whole complex system and cannot be taken as a basis to separate the whole system into two independent subsets of structures and noisy background.

as their large variability (6). Watching such turbulent flows, one recognizes immediately the flow type by its overall structure, but at the same time one gets the impression that over time the exact same patterns are never seen twice. This mutuality of order and stochasticity is one exciting aspect of flow patterns. The two examples selected for this review also nicely reflect this mutuality. One of the challenging problems of turbulence is the small scale-structure and its deviation from Gaussian statistics (cf. 6–8). The anomalous statistics can be seen in connection with the millennium problem, defined by Clay Mathematic Institute, which asks for the local structure of a solution of turbulent flows described by the Navier-Stokes equation (9). An open question is whether there are special small-scale coherent structures explaining the anomalous statistics. For sea waves, coherent structures seem natural; however, we note here that we are not interested in cases of periodic wave structures but in cases of rough seas. A most prominent wave structure of rough seas is the monster wave, which is also called a freak or rogue wave. Still an open question remains whether these structures are part of the disordered wave state or somehow independent of it (cf. 10–12). Turbulent-like features of waves are treated as wave turbulence. This leads to the open problem of

what the basic features of such complex structures are. Questions can be formulated concerning whether there are some clear structures (coherent deterministic structures) that can be singled out to serve as skeletons to access the greater complexity. Alternatively, one may ask whether such systems can be understood best by their stochasticity and statistics? Quite often one approaches such complex systems in a pragmatic way by studying either the structures or the stochasticity.

Another common approach to characterizing such complex patterns is to apply linear correlation measures, because such patterns decay in time or, respectively, in space. Typically for complex systems, like for turbulence, no simple exponential decay of such correlations is found; consequently, we are facing the problem of multiscale correlated systems. Indeed, for such systems low-order statistics, i.e., one-point statistics and two-point correlations, are not sufficient to grasp the observed complexity.

Our present work is different from work devoted to the analysis of nonlinear dynamics with and without noise in the framework of time-series analysis. For time-series analysis, the proper embedding, Lyapunov exponents, fractal dimensions, fixed points, stable and unstable limit cycles, and reconstruction of dynamic equations, etc., are of interest (cf. 5, 14). Although methods of time-series analysis are used, this work focuses on the extended spatial disordered structures with the aim to get a comprehensive characterization at arbitrarily many points, i.e., by general N-point joint statistics. The development of such a method has been stimulated by research on turbulent flows (15), and may be considered a top-down approach. Knowing such a general description, it should be possible to determine all statistical aspects of the system. Furthermore, the common problem of structures versus statistics should be sorted out, as the general N-point joint statistics can grasp any sequential ordering of some patterns as multipoint structures. Also, the mentioned multiscale correlations and higher-order statistics can be captured by general N-point statistics. The question is how complicated such joint statistics become. For the empirical estimation of N-point statistics, the question of whether sufficient data can be provided rises immediately.

For a general approach to N-point statistics, we propose a hierarchical ordering of the N-point statistics. This hierarchical ordering is in analogy to the common cascade picture of turbulence, which describes how structures on larger scales interact with structures on smaller scales in a hierarchical way, so that a downward cascade from large to small scales is obtained. Inspired by the idea of a cascade, we investigate how the scale-dependent structures change with the scale at each location. Vividly interpreted, this can be taken as a zooming-in process of the complex structure. To get access to the highly demanding multipoint statistics, we set the scale dependency of the complex structure in the context of a stochastic process evolving in scale. The novelty is that we do not consider the common time evolution of stochastic processes but an evolution in scale. We show evidence that this zooming-in process can be approximated by a Markov process, i.e., that this process has no long-term memory in its scale evolution. It is this Markov approximation that allows derivation of a Fokker–Planck equation (FPE), evolving in scale, for the hierarchical ordering of the N-point statistics. The FPE is not only a compact description of the whole complexity but also enables derivation of several other aspects ranging from scaling behavior to thermodynamics, as outlined in this review.

This work has its origin in a series of former works started in 1996 (15–17). Initially the idea of a scale-dependent process was worked out without paying much attention to how to nest smaller structures into larger structures, and it can be seen as a continuous formulation of the propagator description of the cascade (18, 19). Reviews of this approach can be found in References 5 and 20, where the stochastic processes in general and the difference between commonly known stochastic processes in time and the new processes in scale are worked out. In Reference 5, applications and citations of stochastic processes in scale are given, which range from turbulent flows, financial data, and surface roughness to earthquakes, cosmic background radiation, and iEEG (intracranial

TAYLOR'S HYPOTHESIS OF FROZEN TURBULENCE

In 1938, G. I. Taylor introduced a hypothesis by which he deduced the spatial fluctuations of a turbulent velocity profile from the corresponding measurements of temporal fluctuations at a single point. This hypothesis, known as the Taylor frozen-flow hypothesis, relies on the existence of a mean flow $\langle u \rangle$ that translates the spatial structures past a stationary probe in a period shorter than the inherent evolution time of the fluctuations (24). $q(x + \mathrm{d}x) \approx q(x - \langle u \rangle \mathrm{d}t)$, where we take the mean flow in the x direction. Therefore, analyses are taken to be equivalent regardless of whether they are taken as a snapshot in space (see **Figure 1**) or as a time sequence of the structures passing over a sensor via the mean flow velocity. Here, we discuss only the spatial complexity.

electroencephalography) recordings from epilepsy patients. All these examples pose remarkable multiscale features, and the complexity seems to be related to a hierarchical ordering connected to cascade-like structures. At this stage, the expression of multipoint and multiscale statistics was used synonymously. With the attempt to reconstruct time series from the knowledge of the multiscale processes (21), the meaning of the correct placement of the smaller-scale structures within the larger ones became clear, and the relationship between multiscale and multipoint statistics has been worked out. In Reference 22, this was done for financial market data and a short-time forecasting has been worked out. For turbulence data (23), it has been realized that an extended class of stochastic cascade processes, expressed by a family of FPEs, is needed. In the present work, we work out in detail the multipoint approach and relate this to the stochastic cascade processes in scale. The technical details for the handling of empirical data is given in corresponding sections.

In our approach, we first consider the simplification of one-dimensional cuts of complex patterns (for turbulence this simplification is related to the Taylor's hypothesis of frozen turbulence—see the sidebar titled Taylor's Hypothesis of Frozen Turbulence). Thus, a quantity $q(x)$ along an axis x is considered. Second, the hierarchical ordering is introduced by changing the scales r, thus we ask what the structure looks like on different scales r, where the changes go from large to small distances, as explained in the next section. Furthermore, we show how the N-point statistics can be expressed by joint multiscale statistics. In Section 3, a three-point approach or three-point closure for the hierarchical multiscale statistics is described, which finally opens the possibility of projecting the general N-point statistics on the stochastic processes in the scale parameter r, ending in a scale-dependent FPE (see Section 4). In Section 5, special self-similar or fractal solutions of the stochastic cascade process are discussed. Two further consequences are deduced from this approach. On one side, we show in Section 6 that surrogate data sets can be produced with the same statistical properties and patterns as in the original processes. On the other side, in Section 7, the stochastic approach is put in the context of nonequilibrium thermodynamics for complex systems, relating complex structures with the integral fluctuation theorem.

2. MULTIPOINT STATISTICS EXPRESSED BY INCREMENT STATISTICS

One important basic aspect of this work is the connection between the general multipoint characterization of a complex structure and its multiscale properties. (See the sidebar titled Multipoint and Multiscale Statistics.) We start with a formal consideration and show how this connection can be worked out mathematically; the sections that follow show consequences and applications. We consider the case in which a complex structure is given as a space and time dependence of a quantity $\vec{q}(\vec{x}, t)$. For the example of a turbulent flow, $\vec{q}(\vec{x}, t)$ is given by a velocity field $\vec{u}(\vec{x}, t)$. For

MULTIPOINT AND MULTISCALE STATISTICS

A clear differentiation between multipoint statistics and multiscale statistics should be made. The multipoint statistics are given by $W(q_0, \ldots, q_N)$. After Equation 4, multipoint statistics can also be expressed in terms of increments ξ_i,

$$W(q_0, \ldots, q_N) \equiv W(\xi_0, \xi_1, \ldots, \xi_{N-1}, q_N).$$

The multiscale statistics are given by

$$W(\tilde{\xi}_0, \tilde{\xi}_1, \ldots, \tilde{\xi}_{N-1})$$

for the scale-dependent quantity $\tilde{\xi}_i(r_i)$, which could be, besides an increment, also another scale-dependent quantity (see the sidebar titled Wavelets, Increments, and Correlations).

When increments $\xi_i = \xi(x_N, r_i)$ are considered for multipoint statistics, the definition of the reference point x_N is of special relevance. Besides the left-jusitified increment $\xi_i^l(x_N, r_i) = q(x_N + r_i) - q(x_N)$, a right-justified definition $\xi_i^r(x_N, r_i) = q(x_N) - q(x_N - r_i)$ can also be used, as we do here. For the multiscale statistics, also a centered version $\xi_i^c(x_N, r_i) = q(x_N + r_i/2) - q(x_N - r_i/2)$ has been used (see References 25 and 26, in which further details on the relationship between these different definitions are given). In this review, we restrict ourselves to the right-justified definition, as this is required for the multipoint reconstruction of data in Section 6.

Note that from the multipoint statistics the multiscale statistics can be derived, but as the reference value q_N is not taken explicitly into account in the multiscale statistics anymore, one cannot derive the multipoint statistics from the multiscale statistics in general (see also References 22 and 23).

a surface, $\vec{q}(\vec{x}, t)$ is the spatial pattern of the height $h(\vec{x}, t)$. As mentioned in the introduction, we simplify this system by assuming that its temporal and spatial structures are statistically similar, and in addition only one direction is of interest. We also assume that the characterizing quantity is a scalar $q(x)$. We are interested in multipoint statistics, i.e., the probability of finding a sequence of events $q(x_i)$ for several discrete locations x_i with $i = 0, \ldots, N$, which is given by the joint probability density function (jPDF),

$$W(q_0, q_1, \ldots, q_N), \qquad 1.$$

where we used the abbreviation $q_i := q(x_i)$. Here, $W(q_0, q_1, \ldots, q_N)dq_0 \ldots dq_N$ is the probability that the random variables $q(x_0), q(x_1), \ldots, q(x_N)$ belong to the intervals $q_0 \le q(x_0) \le q_0 + dq_0, \ldots, q_N \le q(x_N) \le q_N + dq_N$. Instead of this $N+1$-point jPDF W, one may be interested in the conditional probability of obtaining the value q at one selected point under the condition of the remaining events.

In the following, we select the value of q at the last point x_N as a reference value. Therefore, the conditional probability of finding $q(x_N)$ for the given preceding data $q(x_i)$, with $i = 0, \ldots, N-1$, is given by the conditional probability density function (cPDF), which can also be taken as a transition probability,

$$p(q_N|q_0, \ldots, q_{N-1}) = \frac{W(q_0, q_1, \ldots, q_N)}{W(q_0, \ldots, q_{N-1})}. \qquad 2.$$

The multipoint probabilities can also be expressed in another way by considering the statistics of relative changes from one selected point. For x_N as the point of reference, we denote the distance

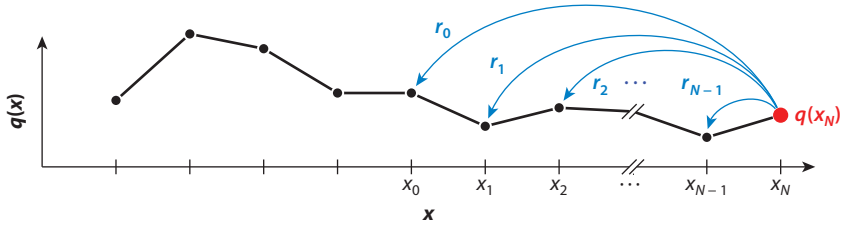

Figure 2

Scheme of the hierarchical ordering of increments $\xi_i = q(x_N) - q(x_N - r_i)$ and scales r_i in order to describe N-point statistics. Sorting the scales after their sizes, from large to small, one obtains a zooming-in process, to which a trajectory $\xi_i(\cdot)$ can be assigned. This process then describes the evolution of the increments ξ_i when scales r_i evolve from largest to smallest size. Abbreviation: TRS, time-reversal symmetry.

or scale $r_i := x_N - x_i$. Therefore, we introduce increments [other notations are common in the literature, such as $\delta_r q(x_i)$, $\Delta q(x_i)$, $q_r(x_i)$, . . .],

$$\xi_i := \xi(x_N, r_i) = q(x_N) - q(x_N - r_i), \qquad 3.$$

for $i = 0, \ldots, N-1$, which quantify the differences of q over the distances or scales r_i, as illustrated in **Figure 2**.

Using the coordinate transformation, $q_i = q_N - \xi_i$, the $N+1$-point jPDF of Equation 1 can be rewritten without loss of information as a jPDF of N increments and the reference value q_N,

$$\begin{aligned} W(q_0, \ldots, q_N)\, dq_0 \ldots dq_N &= W(\xi_0, \xi_2, \ldots, \xi_{N-1}, q_N)\, |J|\, d\xi_0 d\xi_2 \ldots d\xi_{N-1} dq_N \\ &= p(\xi_0, \xi_2, \ldots, \xi_{N-1} | q_N) \cdot W(q_N)\, d\xi_0 d\xi_2 \ldots d\xi_{N-1} dq_N. \end{aligned} \qquad 4.$$

$|J|$ denotes the determinant of the Jacobian for the transformation $(q_0, \ldots, q_N) \to \xi_0, \xi_2, \ldots, \xi_{N-1}, q_N$ and is unity. Here, $W(q_N)$ is the one-point probability density function (PDF) for the value q_N. Based on the natural ordering $x_0 < x_1 < \cdots < x_N$, the scales r_i are ordered as $r_i > r_{i+1}$. Note that we have defined a scale evolution of r_i running with the index i from large to small scale, which can be illustrated as a process in which one zooms in to resolve smaller and smaller structures. For further discussion, see the sidebar titled Wavelets, Increments, and Correlations.

With Equation 4, we have expressed the general $N+1$-point statistics by the statistics of N increments ξ_i taken in a right-justified way from the point q_N. If the statistics of the complex structure are homogeneous (or, for time dependencies, stationary), the probability $W(\xi_0, \xi_2, \ldots, \xi_{N-1}, q_N)$ does not depend on the location x_N but on the values of the describing quantity, here q_N.

3. CLOSURES OF MULTIPOINT STATISTICS

The introduction of the hierarchical ordering of the increments, $\xi_0, \xi_1, \ldots, \xi_{N-1}$, with $r_i > r_{i+1}$ (see **Figure 2**), has been used so far to reformulate the N-point statistics by increment statistics. As a next step, we consider this hierarchical ordering of the increments as scale-dependent fluctuations of the quantity q that go from large to small scales or vice versa. Later on, this becomes an essential aspect for working out a cascade idea for the description of complex systems. Before we get to that

WAVELETS, INCREMENTS, AND CORRELATIONS

The description of the complex structure by multi-increment statistics can be viewed in analogy to a wavelet analysis (cf. 18, 27–29). Wavelets $\psi_{a,b}(x)$ are characterized by a scale a (width) and a location b. Using the difference of two Dirac functions, $\delta(x)$, the scale, $a = r_i$, and the location, $b = x_N$, it is possible to define the following wavelet,

$$\psi_{r_i,x_N}(x) = \delta(x_N - x) - \delta(x_N - r_i - x),$$

also sometimes called the poor man's wavelet. Increments are nothing other than the coefficients of these wavelets,

$$\xi_i = \xi(x_N, r_i) = \int_{-\infty}^{\infty} \psi_{r_i,x_N}(x) q(x) \mathrm{d}x.$$

As discussed in Reference 18, we analyze the evolution of these coefficients of the wavelets with scales as stochastic processes. In principle, the discussion in this review can also be performed with general wavelets $\psi_{r,x}(\cdot)$ and their coefficients $\tilde{\xi}(x, r)$. A main difference is that the increment statistics can be related directly to N-point statistics. For instance, the correlation functions are given by the second-order moment $\langle \xi^2(x, r) \rangle = 2\langle q^2 \rangle - 2\langle q(x - r)q(x) \rangle$. Consequently, higher-order and mixed-order correlations are directly related to higher-order moments of the increment PDF, such as $\langle \xi^n(x, r) \rangle$.

point, some formal aspects of the joint probabilities must be discussed. The jPDF of Equation 4 can be expressed by a product of conditional probabilities,

$$W(\xi_0, \xi_2, \ldots, \xi_{N-1}, q_N) = p(\xi_{N-1}|\xi_{N-2}, \ldots, \xi_0, q_N) \cdot p(\xi_{N-2}|\xi_{N-3}, \ldots, \xi_0, q_N) \cdot \ldots \cdot p(\xi_1|\xi_0, q_N) \cdot p(\xi_0|q_N) \cdot W(q_N). \quad 5.$$

A tremendous simplification arises, if the multiconditioned PDF only depends on the increment of the next larger scale,

$$p(\xi_i|\xi_{i-1}, \ldots, \xi_0, q_N) = p(\xi_i|\xi_{i-1}, q_N). \quad 6.$$

We then obtain a much simpler form of Equation 5, i.e.,

$$W(\xi_0, \xi_1, \ldots, \xi_{N-1}, q_N) = p(\xi_{N-1}|\xi_{N-2}, q_N) \cdot p(\xi_{N-2}|\xi_{N-3}, q_N) \cdot \ldots \cdot p(\xi_0|q_N) \cdot W(q_N). \quad 7.$$

This simplification has two consequences. One one side, this is the basis on which the considered systems can be described by stochastic processes in scales shown in the next section. On the other side, these simplified cPDFs, $p(\xi_i|\xi_{i-1}, q_N)$, are three-point statistics, $p(\xi_i|\xi_{i-1}, q_N) \cdot W(\xi_{i-1}, q_N) \equiv W(q_{i-1}, q_i, q_N)$. Therefore, Equation 7 is a three-point closure of the the general $(N + 1)$-point jPDF. We remark here that possible closures are of central interest for the turbulence problem and that in Reference 30 such a three-point closure is discussed for the Lundgren–Monin–Novikov hierarchy, which is a description of turbulence by multipoint probabilities.

Two further simplifications are given; first, if the cPDFs are independent of the reference q_N (see also the sidebar titled Multipoint and Multiscale Statistics) then

$$p(\xi_i|\xi_{i-1}, q_N) = p(\xi_i|\xi_{i-1}), \quad 8.$$

and second, if the cPDFs are independent of larger increments, then

$$p(\xi_i|\xi_{i-1}, q_N) = p(\xi_i|q_N) \text{ or } p(\xi_i|\xi_{i-1}) = W(\xi_i). \quad 9.$$

The last conditions correspond to a two-point closure for which the general $N+1$-point probability factors completely to products of simple one-increment or one-scale probabilities as

$$W(\xi_0, \xi_1, \ldots, \xi_{N-1}, q_N) = p(\xi_0|q_N) \cdot p(\xi_1|q_N) \cdot \ldots \cdot p(\xi_{N-1}|q_N) W(q_N), \quad 10.$$

$$W(\xi_0, \xi_1, \ldots, \xi_{N-1}) = W(\xi_0) \cdot W(\xi_1) \cdot \ldots \cdot W(\xi_{N-1}), \quad 11.$$

rely on the dependence on q_N. Only for the case that the increment statistics are also independent of the reference value $p(\xi_i|q_N) = W(\xi_i)$, a complete knowledge of the single-increment PDFs $W(\xi_i)$ for all scales completely characterize the multiscale disorder of the considered complex structure; this is an aspect that is important for the fractal characterization of complex structures (see also Section 5). We can conclude that a characterization of a complex system, which is done only by the statistics of increments based on $W(\xi_i)$, is a special two-point characterization. With the knowledge of the PDFs $W(\xi_i)$, all higher-order moments of $\langle \xi_i^n \rangle$ for all scales are known, but nothing is known on more than two-point correlations. Thus, the question of how far the general multipoint problem can be reduced is of central importance for the proper characterization of complex systems.

The validity of the simplifications can be tested with data from concrete complex systems. As we focus in this contribution on the reduction to three-point statistics (see Equation 6), the validity of the simplification can be seen by investigating $p(\xi_i|\xi_{i-1}, \ldots, \xi_0)$. This is easily done by determining different increments for the same reference value q_N. As an example, the results from one turbulent data set is shown in **Figure 3**. Here the quantity of the system is the local velocity in the direction of the mean flow, thus $q_i = u_i$. Clearly $p(\xi_3|\xi_2, \xi_1)$ depends on ξ_2, as the contour lines are not parallel to the ξ_2 axis. Thus, the simplification of Equation 9, namely the reduction to two-point statistics, does not hold. It can, however, be seen that the double-cPDF, $p(\xi_3|\xi_2, \xi_1)$, is similar to the single-cPDF, $p(\xi_3|\xi_2)$. This result is a good indication that Equation 6, the three-point closure, holds. If many data are available, conditions on further larger-scale increments can be investigated. The quality of how well this condition is fulfilled can be tested by statistical tests (see, for example, References 15 and 31) and has been found for many data sets of turbulence (32–34) as well as for other data like financial data (e.g., 22) and surface heights (e.g., 5). In Reference 23, it is shown that this simplification $p(\xi_3|\xi_2, \xi_1, q_N) = p(\xi_3|\xi_2, q_N)$ holds for turbulent data; furthermore, $p(\xi_3|\xi_2, q_N)$ depends on the referee value q_N, too. (Another way of showing Equation 6 for experimental data is given by Reference 35). Note that sometimes we observe that both $p(\xi_3|\xi_2, \xi_1, q_N) = p(\xi_3|\xi_2, q_N)$ and $p(\xi_3|\xi_2, \xi_1) = p(\xi_3|\xi_2)$ hold, but how these Markov conditions are related is not a trivial point. As mentioned for turbulence, the Markov properties are found for both the multipoint $p(\xi_3|\xi_2, \xi_1, q_N)$ and the multiscale $p(\xi_3|\xi_2, \xi_1)$ statistics. For surface waves, we found that Markov properties are only valid for the multipoint statistics (36). If the joint probabilities $W(\xi_3, \xi_2, \xi_1, q_N)$ can be written as $W(\xi_3, \xi_2, \xi_1, q_N) = W(\xi_3, \xi_2, \xi_1) W(q_N)$, then one Markov property always follows from the other.

4. FOKKER–PLANCK EQUATION IN SCALE

So far the characterization of complex disordered structures by multipoint and multiscale statistics has been discussed, as well as has the possible simplifications of three- and two-point closures.

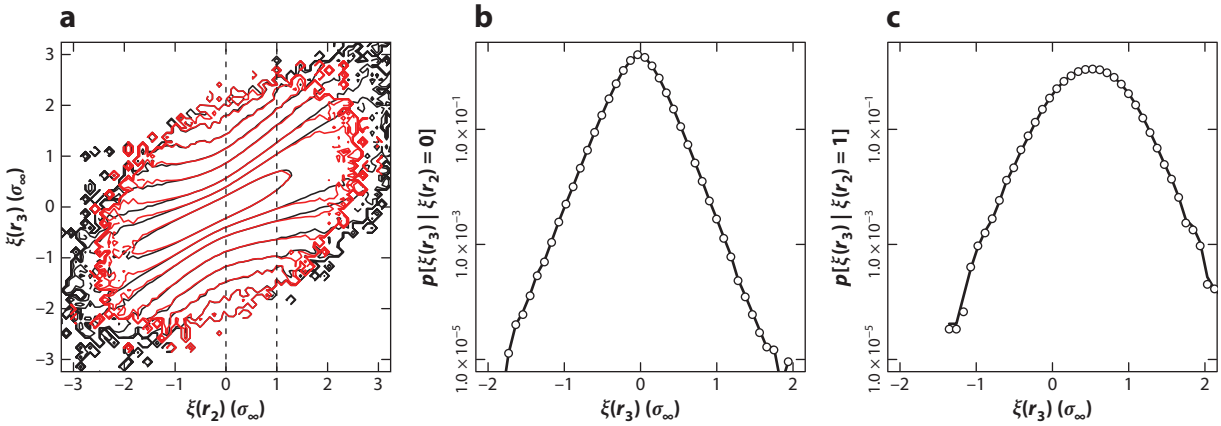

Figure 3

Visualization of Markov properties for velocity increments $\xi(r)$ in a turbulent flow with a Taylor microscale of $\lambda = 0.0024$ m, generated by data of a fractal grid turbulence. Here, the scales r_i of the increments are $r_1 = 3\lambda$, $r_2 = 2\lambda$, and $r_3 = \lambda$. (*a*) Contours of single- and double-cPDFs $p(\xi(r_3)\,|\,\xi(r_2))$ (*black*) and $p(\xi(r_3)\,|\,\xi(r_2), \xi(r_1) = 0)$ (*red*). Cuts at $\xi(r_2) = 0$ and $\xi(r_2) = 1$ are marked by vertical dashed lines. (*b*,*c*) Cuts of panel *a* at $\xi(r_2) = 0$ and $\xi(r_2) = 1$. Single-cPDFs $p[\xi(r_3)\,|\,\xi(r_2)]$ are shown as solid lines, and double-cPDFs $p[\xi(r_3)\,|\,\xi(r_2), \xi(r_1) = 0]$ are shown as as symbols. σ_∞ is the standard deviation of the velocity values u_i, or, respectively, q_i. The cPDF shows two points clearly. First, the dependency on the condition is seen in panel *a* by the change with *x* axis; this shows that $p[\xi(r)\,|\,\xi(r')] \neq p[\xi(r)]$ or that a two-point closure is not supported. Features of the increments for only one selected scale, done by investigating structure functions (see Equation 24), are incomplete. Second, the cPDFs do not depend on a second condition on an increment on an even larger scale r'', $p[\xi(r)\,|\,\xi(r'), \xi(r'')] = p[\xi(r)\,|\,\xi(r')]$. This is taken as an indication that the r evolution of the increments is memoryless; i.e., the knowledge of the value of the increment $\xi(r)$ suffices to determine the next step by which the system evolves to $\xi(r')$, with $r'' < r' < r$. Abbreviation: cPDF, conditional probability density function.

Next, the hierarchical ordering of the increments shown in **Figure 2**, together with the simplification of a three-point closure, which is achieved by Equation 6, is put in the context of cascade processes; we work out a description by stochastic differential equations for this below. Thus, the aim is to grasp the whole complexity by some stochastic equations.

The basic first idea is to look at the increment for a chosen location x_N, i.e., $\xi(x_N, r_i)$ as a quantity that changes with r, and denote it by the increment trajectory $\xi(\cdot) \equiv \xi(x_N, r)$, which describes the above-mentioned zoom-in process. Equation 6 is now nothing other than that $\xi(x_N, r_i)$ depends only on the increment of the next larger scale $\xi(x_N, r_{i-1})$. At the same time, $\xi(x_N, r_i)$ is independent of further increments on larger scales. This means that the evolution of $\xi(\cdot)$ has no memory. Note, this is the definition of a Markov process in scale r. Thus, this evolution has Markov properties and can be considered a stochastic process evolving in r or, more precisely, based on our definition, evolving with decreasing r. [For readers who are not familiar with stochastic processes, see the sidebar titled Markov Process: Fokker–Planck, Kolmogorov, and Langevin Equations and the continuing literature (37–39); see also the sidebar titled Comments on Markov Processes.]

For experimental or empirical data like that from turbulence or from financial markets (41), the absence of memory gets lost for the smallest scales. Such behavior has already been proposed as natural by Einstein in his pioneering work on Brownian motion (42). This defines a lower-bound scale, which we call Einstein–Markov length r_{EM} and which can be determined by the validity of Equation 6 as x_{N-2} converges against x_{N-1} (34). Thus our consideration is valid for $r > \Delta_{\mathrm{EM}}$ and may be treated as a small-scale cutoff (see, e.g., 43). Note that r_{EM} is more than a lower bound, but it is also the finite step size that causes a coarse-gained structure of the whole r evolution

MARKOV PROCESS: FOKKER–PLANCK, KOLMOGOROV, AND LANGEVIN EQUATIONS

For a process of the quantity ξ_i running from large to small scales, i.e., $i = N - 1$ to 0 with $r_i > r_{i+1}$, the Markov processes are defined by the condition that

$$p(\xi_i|\xi_{i-1}; \xi_{i-2}; \ldots; \xi_0) = p(\xi_i|\xi_{i-1}).$$

This means that a cPDF depends only on the value ξ_{i-1} at the closest scale. For such Markov processes, we can write

$$W(\xi_i; \ldots; \xi_0) = p(\xi_i|\xi_{i-1})W(\xi_{i-1}; \ldots; \xi_0).$$

(Note that the discussion presented here is in the same way valid if the reference value q_N is taken into account, too.) Using the same argument for $W(\xi_{i-1}; \ldots; \xi_0)$, we find the following relation for the $i + 1$-point jPDF of Markov processes,

$$W(\xi_i; \ldots; \xi_0) = p(\xi_i|\xi_{i-1}) \ldots p(\xi_1|\xi_0)W(\xi_0).$$

Therefore, marginal PDF $W(\xi_1)$ and cPDF $p(\xi_k|\xi_{k-1})$ are sufficient to describe Markov processes. The probability distributions (marginal and conditional) of Markov processes satisfy a partial differential equation of order one in the scale and order infinity in the state variable ξ. The governing equation is known as the Kramers–Moyal (KM) equation (see Equation 14).

In this respect, the Pawula theorem states that there are only three possible cases in the KM expansion:

(*a*) The KM expansion stops at $n = 1$ means that the processes are deterministic;
(*b*) the KM expansion stops at $n = 2$ means the resulting equation is the Fokker–Planck or Kolmogorov equation and describes diffusion processes; and finally
(*c*) the KM expansion stops at $n = \infty$ means that any truncation of expansion at finite order $n > 2$ would produce nonpositive probability density $W(\xi)$ (37).

For case b, the KM expansion reduces to the FPE, which means that the first and second KM coefficients $D^{(1)}(\xi, r)$ (drift coefficient) and $D^{(2)}(\xi, r)$ (diffusion coefficient) are nonvanishing (see Equations 15 and 16). One can ask which dynamical equation governs the stochastic variable ξ itself, where its marginal and conditional PDFs satisfy the FPE. The corresponding stochastic equation is known as the Langevin equation. Using the Itô interpretation, it has the following form (5):

$$-r\frac{\mathrm{d}\xi}{\mathrm{d}r} = D^{(1)}(\xi, r) + \sqrt{D^{(2)}(\xi, r)}\eta(r),$$

where noise $\eta(r)$ is a zero-mean, white-noise Gaussian with intensity 2, which means that $\langle \eta(r)\eta(r')\rangle = 2\delta(r - r')$.

from largest to smallest scale. In this way, the Markov process may be taken as a stochastic process modeling the coarse-grained process in a continuous manner.

The evolution of the cPDFs $p(\xi|\xi_i, q_N)$ with $r < r_i$ describes the transition probability of $\xi_i(r_i) \to \xi(r)$ for the given reference q_N. An equation for the evolution of this transition probability, and extending the difference between r and r_i, is given by the Kramers–Moyal (KM) expansion (more precisely, the KM forward expansion) (37),

$$-r\frac{\partial}{\partial r}p(\xi|\xi_i, q_N) = \sum_{n=1}^{\infty}\left(-\frac{\partial}{\partial \xi}\right)^n \left[D^{(n)}(\xi, r, q_N)p(\xi|\xi_i, q_N)\right]. \qquad 14.$$

COMMENTS ON MARKOV PROCESSES

Direction of the Process

The evolution of the scales from large to small values is considered; for this purpose, we used in Equation 14 a negative prefactor of $-r$. Having $-r/\partial r = -1/\partial ln(r)$ shows that we have implicitly used a log scaling of the r evolution, which is advantageous for complex structures with self-similar properties (see Section 5).

Inverse Direction of the Process

If it is shown that the data fulfill the Markov conditions of Equation 6 from large to small scales, the Markov condition is fulfilled also in the other direction, from small to large scales (40):

$$p(\xi_i|\xi_{i+1},\ldots,\xi_{N-1},q_N) = p(\xi_i|\xi_{i+1},q_N) \qquad 12.$$

as

$$\begin{aligned} p(\xi_i|\xi_{i+1},\ldots,\xi_{N-1},q_N) &= \frac{W(\xi_i,\xi_{i+1},\ldots,\xi_{N-1},q_N)}{W(\xi_{i+1},\ldots,\xi_{N-1},q_N)} = \frac{W(\xi_{N-1},\xi_{N-2},\ldots,\xi_i,q_N)}{W(\xi_{N-1},\xi_{N-2},\ldots,\xi_{i+1},q_N)} \\ &= \frac{p(\xi_{N-1}|\xi_{N-2},q_N)\ldots p(\xi_{i+2}|\xi_{i+1},q_N)\; p(\xi_{i+1}|\xi_i,q_N)W(\xi_i,q_N)}{p(\xi_{N-1}|\xi_{N-2},q_N)\ldots p(\xi_{i+2}|\xi_{i+1},q_N)W(\xi_{i+1},q_N)} \\ &= \frac{W(\xi_{i+1},\xi_i,q_N)}{W(\xi_{i+1},q_N)} = p(\xi_i|\xi_{i+1},q_N). \end{aligned} \qquad 13.$$

$D^{(n)}$ are called KM coefficients (see the sidebar titled Higher-Order Kramers–Moyal Coefficients) and can be found from time series (see below). If the fourth-order KM coefficient $D^{(4)}$ vanishes, the KM expansion reduces after Pawula's Theorem (cf. 37; see the sidebar titled Markov Process: Fokker–Planck, Kolmogorov, and Langevin Equations) to an FPE, which is also known as the Kolmogorov equation (44). For the FPE, the expansion of Equation 14 truncates after the second term,

$$-r\frac{\partial}{\partial r}p(\xi|\xi_i,q_N) = -\frac{\partial}{\partial \xi}\left[D^{(1)}(\xi,r,q_N)p(\xi|\xi_i,q_N)\right] + \frac{\partial^2}{\partial \xi^2}\left[D^{(2)}(\xi,r,q_N)p(\xi|\xi_i,q_N)\right]. \qquad 15.$$

Note that if $p(\xi|\xi_i,q_N)$ is independent on q_N and if one multiplies the equation with $W(\xi_i)$ and integrates over ξ_i, Equation 15 reduces to [here $W(\xi) = \int p(\xi|\xi_i)W(\xi_i)\mathrm{d}\xi_i$]

HIGHER-ORDER KRAMERS–MOYAL COEFFICIENTS

According to the Pawula theorem, vanishing higher-order KM coefficients, especially fourth-order $D^{(4)}(\xi,r)$, guarantee that the process is statistically continuous, and the KM expansion Equation 14 can be truncated after the second (diffusive) term (cf. 37). For vanishing (higher-order $n > 2$) KM coefficients, one can construct the Langevin equation with the computed drift function and diffusion coefficients form time series. Nonvanishing higher-order ($n > 2$) KM coefficients have been observed in various systems (cf. 5), which indicates that the corresponding measured time series do not belong to the class of continuous diffusion processes and that jump events should play a significant role in the underlying stochastic process (45).

$$-r\frac{\partial}{\partial r}W(\xi) = -\frac{\partial}{\partial \xi}\left[D^{(1)}(\xi,r)W(\xi)\right] + \frac{\partial^2}{\partial \xi^2}\left[D^{(2)}(\xi,r)W(\xi)\right], \quad 16.$$

which leads to the pure description of the increment statistics of $W(\xi)$. This is clearly less information than $p(\xi|\xi_i)$, which we know from the discussion of the multipoint statistics in the previous section. Note that $D^{(n)}(\xi,r,q_N)$ and $D^{(n)}(\xi,r)$ are related by $\int D^{(n)}(\xi,r,q_N)p(\xi|\xi_i,q_N)W(q_N)\mathrm{d}q_N = D^{(n)}(\xi,r)p(\xi|\xi_i)$.

Looking at the evolution of the increments ξ_r with scale, the Markov property of Equation 6 means that only delta-correlated noise acts on the trajectory. The reduction of the KM expansion of Equation 14 goes along with the requirement that the involved noise in the stochastic process is not only delta correlated but has also Gaussian distribution. This is also called Langevin noise, for which a corresponding differential equation for a single event or path $\xi(\cdot)$ is given as

$$-r\frac{\partial}{\partial r}\xi = D^{(1)}(\xi,r) + \sqrt{D^{(2)}(\xi,r)}\eta(r), \quad 17.$$

where $\eta(r)$ denotes zero-mean, Gaussian white noise with a variance of 2; i.e., $\langle\eta(r)\eta(r')\rangle = 2\delta(r-r')$. Here, we use the Itô interpretation. For Stratonovich and other descriptions, see References 37 and 38. From the Langevin equation, it is evident that $D^{(1)}$ describes the deterministic part of this equation and is called the drift coefficient. The function $D^{(2)}(\xi,r)$, which is called the diffusion coefficient, determines the amplitude of the noise. The case that $D^{(2)}$ changes with ξ is called multiplicative noise.

An essential point for the stochastic description of the scale-dependent increments is the knowledge of the KM coefficients $D^{(n)}$, which can be determined directly from the data as conditional moments (cf. 5, 37).

First, let us define the nth-order moments for two increments in scales that are separated by δ:

$$\begin{aligned} M^{(n)}(\delta,\xi,r,q_N) &= \left\langle\left[\xi'(r-\delta,q_N)-\xi(r,q_N)\right]^n\right\rangle|_{\xi(r,q_N)=\xi} \\ &= \int_{-\infty}^{\infty}\left(\left[\xi'(r-\delta,q_N)-\xi(r,q_N)\right]^n\right)p(\xi'|\xi,q_N)d\xi'. \end{aligned} \quad 18.$$

The values of $M^{(n)}$ depend on the value of δ for some chosen or fixed values of ξ, r, and q_N. The KM coefficients $D^{(n)}$ are given by

$$D^{(n)}(\xi,r,q_N) = \frac{r}{n!}\lim_{\delta\to 0}\frac{1}{\delta}M^{(n)}(\delta,\xi,r,q_N). \quad 19.$$

The definition presented here for KM coefficients differs by the factor of r from common definition, which is due to our description of a stochastic process in scale (see Equation 17). It should be mentioned that this definition of the KM coefficient can already be found in an early work of Kolmogorov's in 1931 (44).

We see that the cPDFs, $p(\xi'|\xi,q_N)$, play again an important role, as for the $\lim_{\delta\to 0}$ the differential Equation 14 can be estimated from their knowledge. Note that this $\lim_{\delta\to 0}$ can be considered a fusion process of two increments $\xi_j' \to \xi_j$, which is of interest for a field theoretical approach to such complex systems (5, 30, 46, 47).

An important aspect of Equations 18 and 19 is that they can also be read as a concept to estimate the KM coefficients directly from given data, as shown for some turbulence data in **Figure 4**. This

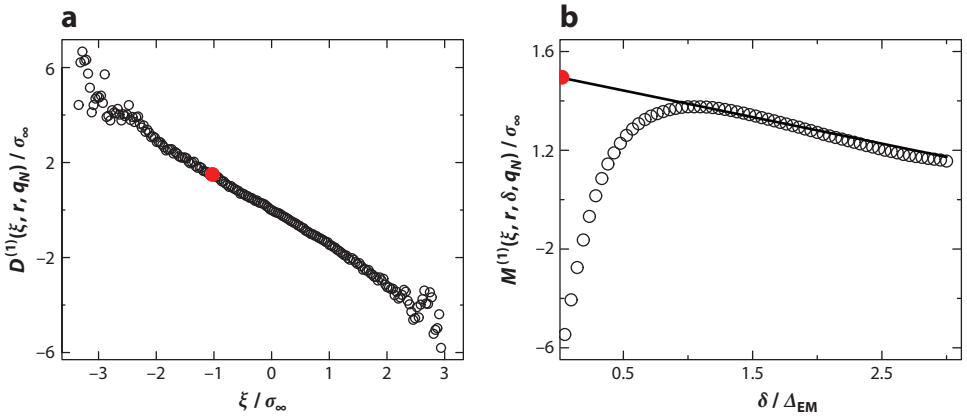

Figure 4

The scheme for how Kramers–Moyal coefficients can be determined using Equation 19 is illustrated for the first Kramers–Moyal coefficient or drift term. (*a*) The drift term for a turbulent flow. (ξ is normalized to σ_∞, the variance of the signal itself.) The red dot of $D^{(1)}$ marks a value for which the conditional moment $M^{(1)}(\xi, r, \delta, q_N)$ is evaluated (see panel *b*). The function $D^{(1)}(\xi, r, q_N)$ is obtained point by point using a linear extrapolation of $M^{(1)}(\xi, r, \delta, q_N)$ for $\lim_{\delta \to 0}$, shown as a solid line (in panel *b*). (Δ_{EM} is the Einstein–Markov length, below which the process is not any more Markovian.) Note that the linear shape of $D^{(1)}$ reflects the deviation of a conditional point density function from the diagonal shown in **Figure 3*a***, and indicates, for the evolution of the increments, after Equation 17, that their sizes decrease as the scales r become smaller. (Data taken from Reference 31.)

was shown to be a very efficient method for analyzing time series of noisy dynamical systems in Reference 5. Experiences have shown that technically the limit $\lim_{\delta \to 0}$ is best performed by investigating the moments $M^{(n)}(\xi, r, \delta, q_N)$ with the help of the small-step approximation in δ, for which $M^{(n)}(\xi, r, \delta, q_N) = D^{(n)}(\xi, r, q_N)\delta + \mathcal{O}(\delta^2)$ (see **Figure 4*b***). If the given data do not allow this small-step approximation, owing to insufficient sampling rates or a too large Einstein–Markov length, respective corrections can be calculated (48, 49). In **Figure 4*b***, the sampling rate was sufficiently high. The deviation from a linear law for small values δ is due to the Einstein–Markov length. Other corrections arise, if additionally measurement or observation noise or another nonideal noise contribution is given (cf. 50–53).

In **Figure 5**, the KM coefficients are shown for a turbulent data set. The linear behavior of the drift term $D^{(1)}$ and the quadratic behavior of the diffusion term $D^{(2)}$ becomes clear. $D^{(2)}$ has an additional additive offset. The fourth-order KM coefficient can be taken as zero within the experimental precision. This indicates that for turbulence an FPE can be used to describe the cascade process and, thus, the whole multipoint statistics. For the case that $D^{(4)}$ does not become zero, in principle infinitely many KM coefficients have to be determined. A criterium to quantify the importance of higher-order KM coefficients has been worked out in Reference 31, and in Reference 33 it has been shown for turbulence that, in contrast to the velocity fields, the passive scalars require such higher-order KM coefficients. Another aspect of the results for the KM coefficients shown in **Figure 5** is that the dependency on the reference point q_N is only clearly present for $D^{(1)}$. For positive q_N, the fixed point $D^{(1)}(\xi) = 0$ is shifted to negative values, whereas for negative q_N the fixed point is shifted to positive values. This result simply means that for positive q_N the increments have the tendency to become more negative, which is in accordance with the boundedness of turbulent velocity data from stationary experiments.

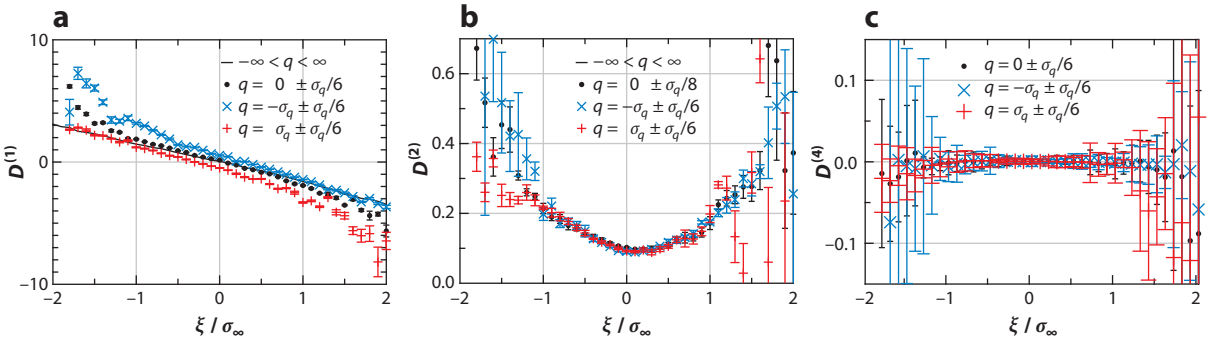

Figure 5

(*a*) First-, (*b*) second-, and (*c*) fourth-order Kramers–Moyal coefficients $D^{(n)}(\xi, r, q_N)$ calculated from data of a turbulent flow, using the procedure illustrated in **Figure 4**. Three different reference values q_N, labeled as $q = -\sigma_q \pm \sigma_q/6$, $q = 0 \pm \sigma_q/6$, and $q = \sigma_q \pm \sigma_q/6$, were chosen. To get sufficient data for the statistics, a small but finite interval around the q_N values was chosen. Here σ_q is the standard deviation of $W(\xi)$. Note that only $D^{(1)}(\xi, r, q_N)$ shows clear dependence on q_N. For further details, see Reference 23. The negative values for the fourth-order Kramers–Moyal coefficient are due to the extrapolation procedure as indicated in **Figure 4**. Once these Kramers–Moyal coefficients are successfully estimated as in this figure, the corresponding Fokker–Planck equation is completely obtained. Figure adapted from Reference 23.

Knowing the coefficients $D^{(1)}$ and $D^{(2)}$, the cPDF $p(\xi_r|\xi_{r+\delta})$ [as well as $p(\xi_r|\xi_{r+\delta}, q_N)$] can be calculated by the short time propagator (31, 37),

$$p_{STP}(\xi_r|\xi_{r+\delta}) \approx \frac{1}{\sqrt{4\pi\ D^{(2)}(\xi_{r+\delta})\ \delta}} \times \exp\left[-\frac{[\xi_r - \xi_{r+\delta} - D^{(1)}(\xi_{r+\delta})\delta]^2}{4D^{(2)}(\xi_{r+\delta})\delta}\right]. \quad 20.$$

A sufficiently small step δ has to be used to stay in this limiting approximation. Based on this short time propagator any cPDF $p(\xi_r|\xi_{r'})$ can be determined. Therefore, the quality of the estimation of the coefficients $D^{(1)}$ and $D^{(2)}$ can be verified by comparing the cPDFs obtained from the data with those obtained by solving the FPE with the estimated coefficients (54).

5. SELF-SIMILARITY AND FRACTALS

In Section 4, we completed the derivation of an FPE as a model of scale-dependent complexity. We now want to put this approach in the context of other analysis frameworks for complex systems, namely self-similarity and fractals. For complex structures, the question is often posed as to whether they possess self-similar structures, i.e., fractals. Particularly for the two examples of turbulence and sea waves discussed here, the concept of self-similarity plays an important role (cf. 6, 10). We start the discussion of self-similarity in a general way with the principles of scaling symmetries, from which we derive properties of the so-called structure functions $\langle \xi^n \rangle$. The structure functions are often used for the characterization of both turbulence and surface roughness like sea waves. We show how the concept of the stochastic cascade equations of the previous section can describe these structure functions and their similiar structure.

Commonly the self-similarity is investigated by a local measure, which characterizes the structure on the scale r at the location x. We denote the local measure again as $\xi(x,r)$. Self-similarity means that in a certain range of r the quantities

$$\xi(x,r) \quad \text{and} \qquad \lambda^{\alpha}\xi(\lambda r, \lambda^{\beta}x) \tag{21.}$$

should have the same statistics, where α and β are scaling exponents. More precisely, the probability distribution of the quantity ξ takes the form

$$W(\xi,r) = \frac{1}{r^{\alpha}}F\left(\frac{\xi}{r^{\alpha}}\right) \tag{22.}$$

with a universal function $F(Q)$. The universality of F leads to the scaling behavior,

$$\langle \xi^k(r)\rangle = \int \xi^k \frac{1}{r^{\alpha}}F\left(\frac{\xi}{r^{\alpha}}\right) \quad \mathrm{d}\xi = Q_k r^{k\alpha}. \tag{23.}$$

Such a type of behavior has been termed fractal scaling behavior.

The concept of fractals is widespread and many examples are known, like turbulence or surface roughness, just to mention two. The strict self-similarity expressed by Equation 21 is often just an idealized approximation. In fact, the so-called multifractal behavior is often more appropriate. Here the kth-order moments scale according to

$$\langle \xi^k(r)\rangle = Q_k r^{\zeta(k)}, \tag{24.}$$

where the scaling indices $\zeta(k)$ are no longer linear but rather a nonlinear function of the order k.

Such a multifractal behavior can formally be obtained by the assumption that the probability distribution $W(\xi,r)$ has the following form:

$$W(\xi,r) = \int \tilde{W}(\alpha,r)\frac{1}{r^{\alpha}}F\left(\frac{\xi}{r^{\alpha}}\right)\,\mathrm{d}\alpha. \tag{25.}$$

This formula is based on the idea that the complex system is composed of subsets of different scaling indices α, where $\tilde{W}(\alpha,r)$ gives a measure of the scaling indices α at a scale r (see, e.g., 19, 55). A shortcoming of the fractal and multifractal approach to complexity in scale is the fact that it only addresses the statistics of the measure $\xi(x,r)$ at a single scale r. As we have derived above, one must expect for a general N-point characterization dependencies of the measures $\xi(x,r)$ and $\xi(x,r')$ from different scales, as well as dependencies in the value of a reference point $q(x)$.

The connection between the fractal and multifractal characterization and the stochastic cascade description can be derived from the KM expansion of Equation 14. The validity of the Markov property or, respectively, the three-point closure, is assumed, and Equation 14 has been integrated over all values of q_N so that the dependency on the reference value is not taken into account anymore:

$$-r\frac{\partial}{\partial r}p(\xi|\xi_i) = \sum_{n=1}^{\infty}\left(-\frac{\partial}{\partial \xi}\right)^n \left[D^{(n)}(\xi,r)p(\xi|\xi_i)\right]. \tag{26.}$$

Multiplying this equation with ξ^k and the partial integration over ξ (e.g., 31) leads to

$$-r\frac{\mathrm{d}}{\mathrm{d}r}\langle(\xi_r)^k\rangle = \sum_{n=1}^{k-1}\frac{k!}{(k-n)!}\langle D^{(n)}\xi_r^{k-n}\rangle. \qquad 27.$$

If the KM coefficients have the form $D^{(n)} = d_n\xi^n$ (where d_n are constants) (56), then scaling behavior of Equation 24 is guaranteed with

$$\zeta_k = -\sum_{n=1}^{k-1}\frac{k!}{(k-n)!}d_n. \qquad 28.$$

Based on this formula, we can deduce which combinations of d_n will result in the q-dependent function of ζ_q, which characterizes different multifractal models.

For turbulence and increments, $\langle(\xi_r)^k\rangle$ is a common quantity to characterize different flow situations. $\langle(\xi_r)^k\rangle$ is called the k-order structure function. If the KM expansion truncates to an FPE, the structure functions can be found from the following equation:

$$-r\frac{\partial}{\partial r}\langle\xi_r^k\rangle = k\langle\xi_r^{(k-1)}D^{(1)}(\xi_r)\rangle + k(k-1)\langle\xi_r^{(k-2)}D^{(2)}(\xi_r)\rangle. \qquad 29.$$

From **Figure 4**, the drift coefficient has a linear behavior, $D^{(1)}(\xi_r) = d_{11}\,\xi_r$, and the diffusion coefficient has a quadratic behavior, $D^{(2)}(\xi_r) = d_{20} + d_{22}\,\xi_r^2$. The d_{ij} may be r dependent. The scaling index now becomes

$$\begin{aligned}\zeta_k &= \frac{r}{\langle\xi_r^k\rangle}\frac{\partial\langle\xi_r^k\rangle}{\partial r} = \frac{\partial\ln(\langle\xi_r^k\rangle)}{\partial\ln(r)}\\ &= -k\left\{d_{11}(r) + (k-1)\left[d_{22}(r) + \frac{\langle\xi_r^{k-2}\rangle}{\langle\xi_r^k\rangle}d_{20}(r)\right]\right\}. \qquad 30.\end{aligned}$$

Due to the additive term in $D^{(2)}(\xi_r)$, a mixing of different structure functions with different orders takes place. For the case of $d_{20} = 0$, which is not supported by experimental data (see **Figure 3**), and for constant values of d_{11} and d_{22}, the so-called Kolmogorov 1962 (K62) or lognormal model (57) is obtained with the intermittency parameter μ,

$$\begin{aligned}\zeta_k &= -kd_{11} + k(k-1)d_{22}\\ &= \frac{k}{3} - \mu\frac{k(k-3)}{18}. \qquad 31.\end{aligned}$$

Thus, the K62 scaling corresponds to $d_{11} = -\frac{3+\mu}{9}$ and $d_2 = \frac{\mu}{18}$. The corresponding relation between stochastic processes and the other well-known multifractal scaling models of turbulence has been worked out in References 30 and 58.

6. SURROGATE DATA AND FORECASTING

The FPE derived in Section 4, despite its compactness, achieves a comprehensive and powerful characterization and description of a wide range of complex systems. However, the generation of

surrogate data that fully obey a special FPE is not trivial. This section develops an approach to this task.

Based on the relationship of the general N-point statistics of a complex structure and a stochastic description by an FPE, we obtain the possibility to generate new data sets numerically or to forecast special events. Therefore, we consider the case that preceding values $q_0, \ldots, q_{N-1}$ fix the probability of a new value q_N. Taking this row of values q_i, where $i = 0, \ldots, N-1$ as a sequence of events, the cPDF of Equation 2 can be seen as the prediction of the next event for the next time step (see, e.g., 59). Such a predictor can be expressed by the stochastic cascade process using Equations 4 and 7,

$$\begin{aligned} p(q_N|q_{N-1},\ldots,q_0) &= \frac{W(\xi_0,\xi_1,\ldots,\xi_{N-2},\xi_{N-1},q_N)}{W(\xi_0,\xi_1,\ldots,\xi_{N-2},q_{N-1})} \\ &= \frac{p(\xi_{N-1}|\xi_{N-2},q_N)\cdot p(\xi_{N-2}|\xi_{N-3},q_N)\cdot\ldots\cdot p(\xi_0|q_N)\cdot W(q_N)}{p(\xi_{N-2}|\xi_{N-3},q_{N-1})\cdot p(\xi_{N-3}|\xi_{N-4},q_{N-1})\cdot\ldots\cdot p(\xi_0|q_{N-1})\cdot W(q_{N-1})} \\ &= \frac{\prod_{i=1}^{N-1} p(\xi_i|\xi_{i-1},q_N)}{\prod_{i=1}^{N-2} p(\xi_i|\xi_{i-1},q_{N-1})} \times \frac{p(\xi_0|q_N)}{p(\xi_0|q_{N-1})} \times \frac{W(q_N)}{W(q_{N-1})}. \end{aligned} \quad 32.$$

Note that the increments ξ_i, defined in Equation 3, must be taken from the reference value q_N in the nominators and from reference value q_{N-1} in the denominators, respectively.

Equation 32 enables us to determine the probability of the new value q_N based on the knowledge of the simple cPDFs $p(\xi_i|\xi_j, q_N)$, which can be either calculated from the FPE or estimated directly from the data. As $p(\xi_i|\xi_j, q_N)$ contains only knowledge of three values, q_i, q_j, and q_N of the data, this is again a three- point closure of multipoint statistics.

The conditional probabilities $p(q_N|q_{N-1},\ldots,q_0)$ contain all relevant statistical information of the previous data points for a correct choice of the new value q_N. Choosing now a random value from this distribution, the time series is extended correctly by another point. Shifting the procedure by one step and repeating the same procedure may be used to generate new surrogate time series, which exhibits the correct jPDF for all considered scales. For technical reasons, one should avoid zeros in cPDFs of the denominator of Equation 32. The initial idea for reconstructing time series following this procedure was developed in a similar way for fluid turbulence data (21), and has been used for turbulent data (23), financial data (22), and also sea waves (36). In **Figure 6**, we show two time series of wind speed measurements. The originally measured time series is shown in **Figure 6*a***; a time series obtained by the just mentioned reconstruction method is shown in **Figure 6*b***. The color-coded left part represents the initial conditions of the first N values, $q_0, \ldots, q_{N-1}$, used to start the reconstruction method. As this is a stochastic model, involving a deterministic as well as a random part, the two time series diverge quite fast. But the stochastic content in the sense of multipoint statistics is the same, which can be verified by reanalyzing these surrogate data (22, 23, 36). Another interesting point is that apparently typical structures of a wave pattern could be reproduced by the stochastic method (60), thus it seems that the multipoint approach can capture the statistics as well as coherent structures. This will only work if such structures are based on the special stochasticity, and it will not work if special structures are added to a noisy background.

The method to reconstruct data sets with the conditional probabilities $p(q_N|q_{N-1},\ldots,q_0)$ can also be used for a short time forecast, as was shown for financial data (22) and sea waves (36). In **Figure 7*a***, typical time series of wave heights is shown. Note that the big wave at the end of the time series corresponds to a measured rogue wave. In **Figures 7*d,e***, two selected conditional

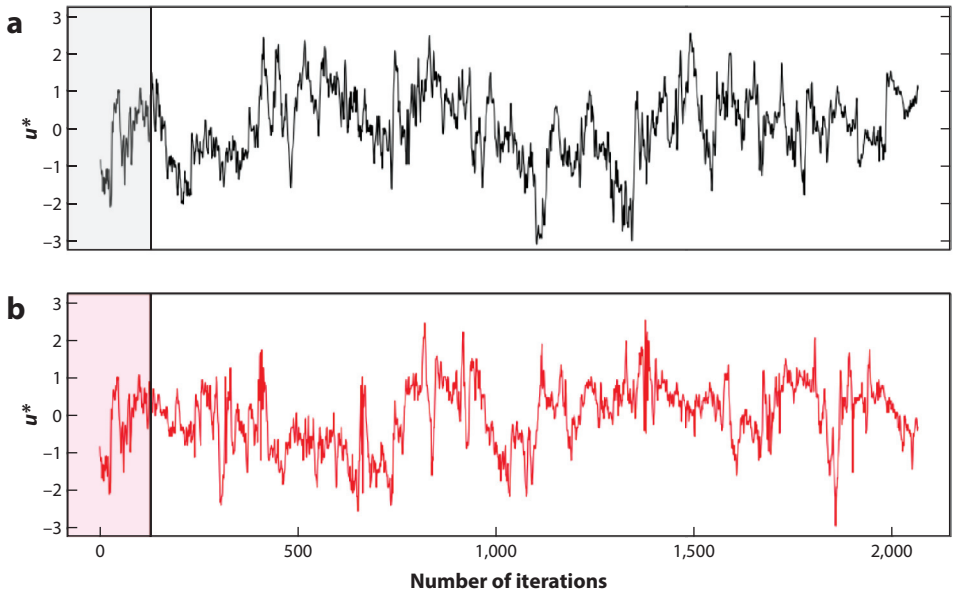

Figure 6

Time series of wind data as a real-world example of numerical data generation (cf. Section 6). Panel *a* shows the measured data, whereas panel *b* presents reconstructed data using Equation 32. The data, which are used as the initial condition for the reconstruction, are marked on the left sides of the panels. The reconstructed data are not identical with the measured data, but they follow the same statistics. Not only mean value and standard deviation but also multipoint statistics and higher-order correlations are correctly reproduced.

probabilities $p(q_N|q_0, r_0, \ldots, q_{N-1}, r_{N-1})$ are shown to illustrate our method. In addition to the conditional probabilities, the single event probability $p(q_N) = p(q)$ of all height values is shown. These figures show clearly how the conditional probabilities change, with $q_0, r_0, \ldots, q_{N-1}, r_{N-1}$, the values of the N wave heights seen before. There are cases when smaller q_N values are expected in the next step (see **Figure 7*b***), and there are cases when large q_N values become highly likely (see **Figure 7*c***). With this method, a warning system for approaching large wave heights can be set up. The high quality of such a prediction was quantified according to the receiver operating characteristic (ROC) curve (36).

7. NONEQUILIBRIUM THERMODYNAMICS OF COMPLEX HIERARCHICAL STRUCTURES

Up to this point, we have outlined a statistical approach to completely characterize the disordered structure in one direction by multipoint statistics. This approach was a phenomenological one. For the case of turbulence, there are some works that show how such an FPE can be related to the basic equations of fluid mechanics. In Reference 61, the connection to the Navier–Stokes equation is shown; in Reference 30, the Lundgren hierarchy was analyzed based on a three-point closure or, respectively, Markov properties in scale. For the sea waves, comparable results are not known to us. In this last section, we put our statistical approach in the context of nonequilibrium thermodynamics (for earlier approaches to nonequilibrium approaches, see, for example,

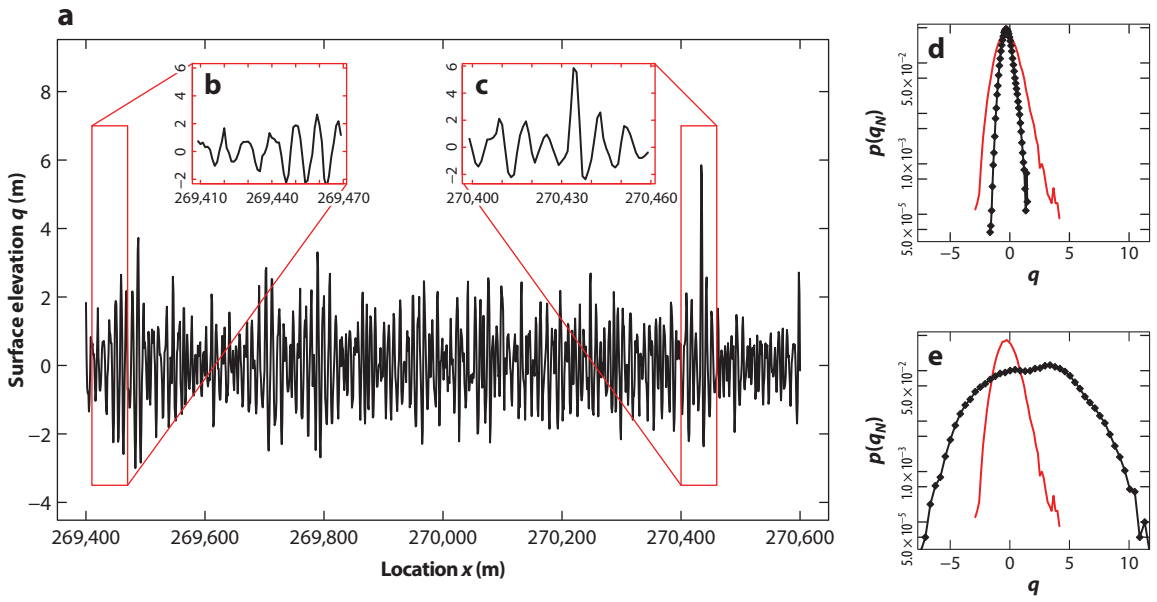

Figure 7

Time series and PDF of ocean gravity waves as a second example of real-world data reconstruction. (*a*) Reconstructed time series using Equation 32. Two time windows are marked as panels *b* and *c*; the corresponding multiconditional PDFs (using Equation 32) are given in panels *d* and *e*. To show the changing volatility, both the multiconditional PDFs (*black*) as well as the unconditional PDFs (*red*), estimated from all data, are shown. Note the obvious changes of the likelihood of large wave amplitudes. The multipoint statistics clearly change along the time series, defining regions of smaller and larger wave amplitudes, respectively. As another aspect, the multiconditional PDFs can serve for short time forecasting. For consistency, the heights of the waves are denoted by the variable q, and the time dependencies have been transformed to a spatial dependency using a wave velocity of 1 m/s. Abbreviation: PDF, probability density function. Data taken from Reference 36.

Reference 62). Based on the derived FPEs for the cascade process, we can assign entropy values to each local structure of the complex systems. For these entropy values, the validity of a fluctuation theorem, namely the integral fluctuation theorem, can be shown. This is how the phenomenological stochastic approach can be linked to fundamental laws of physics (cf. 63).

In particular, the concept of stochastic thermodynamics is applied to turbulent flows (64–66) and sea waves (60). The novelty here is that concepts of nonequilibrium thermodynamics known to hold for microscopic systems are shown to be valid also for such macroscopic systems. These concepts enable us to determine an entropy production of the cascade process. In particular, for every individual trajectory $\xi(\cdot) = \xi_r$, where $r = r_0, \ldots, r_N$ of the increments evolving from large to small scales, a total entropy production ΔS_{tot} can be defined by

$$\begin{aligned}\Delta S_{\mathrm{tot}}\,[u(\cdot)] &= \Delta S_{\mathrm{med}} + \Delta S_{\mathrm{sys}} \\ &= -\int_{r_0}^{r_N} \partial_r \xi_r \partial_\xi \varphi(\xi_r)\,\mathrm{d}r - ln\frac{p(\xi_{r_N}, r_N)}{p(\xi_{r_0}, r_0)}. \end{aligned} \quad 33.$$

The total entropy production is given by the sum of two contributions, with ΔS_{med} being the entropy variation due to the surrounding medium, which depends on the evolution of $\xi(\cdot)$ through the hierarchy of length scales r in the cascade. Here, ΔS_{sys} is the entropy change of the system

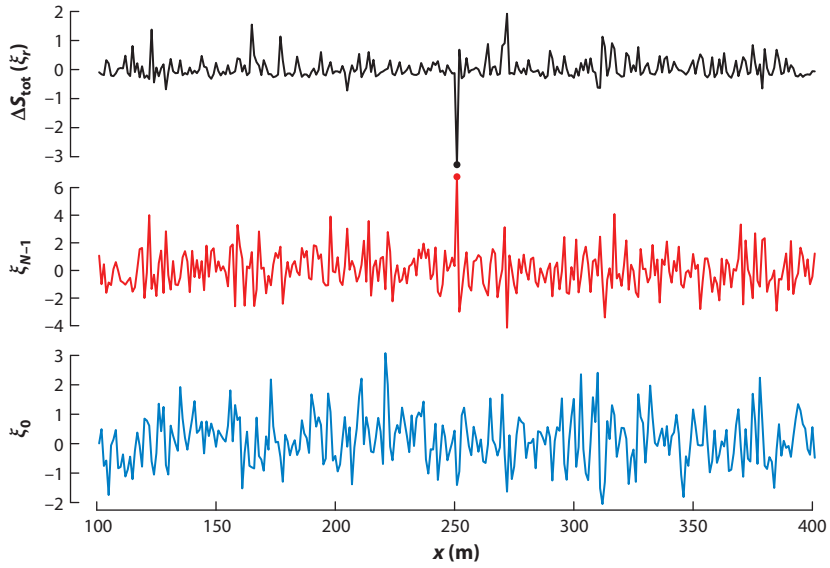

Figure 8

Time series of increments calculated from height values of sea waves together with the corresponding local values of the entropy production (data from Reference 60). Note that for each trajectory of increments one value of the entropy production is obtained. By solid circles the trajectory leading to the highest height increment on small scales is marked and related to the corresponding large negative entropy value. The location on the x axis is given in units of meters, obtained using Taylor's hypothesis with an assumed velocity of 1 m/s. On the y axis the increments for smallest scales are denoted by ξ_{N-1}, and the increments on large scales by ξ_0.

itself. In Equation 33, $\varphi(\xi_r)$ is the potential, which can be obtained from the stationary solution of the estimated FPE,

$$\varphi(\xi_r) = lnD^{(2)}(\xi_r, r) - \int_{-\infty}^{\xi_r} \frac{D^{(1)}(\xi', r)}{D^{(2)}(\xi', r)} \mathrm{d}\xi'. \qquad 34.$$

Dealing with these thermodynamics (see also References 63 and 64), one may interpret $\partial_\xi \varphi[\xi(r)]$ in a less formal way as a force of the medium given by the mean field quantities $D^{(1)}$ and $D^{(2)}$. The interaction of this force on the path velocity $\partial_r \xi_r$ leads then to the entropy term ΔS_{med}, which represents an analog of the work done by the medium on the single event $\xi[\cdot]$, which leads to a heat exchange with the bath (for more details on this analogy, see Reference 67). The second entropy term ΔS_{sys} may be considered an intrinsic contribution of the trajectory. The main point is that to each increment trajectory $\xi[\cdot]$ a value of ΔS_{tot} can be determined like that shown in **Figure 8**. Thus, microscopic entropy fluctuations can be determined, which may show positive and negative values. Interestingly, the negative entropy events are related to extreme events in the increment statistics on the smallest scales, as can be seen in **Figure 8** and as reported in References 60 and 64. This again points in the direction that salient structures of a complex system can be a proper part of the multipoint statistics, somehow unifying the approach to complex systems by coherent structures or by statistical methods. (For a discussion of turbulence, see the sidebar titled Thermodynamical Interpretation of Turbulence.)

THERMODYNAMICAL INTERPRETATION OF TURBULENCE

Entropy values for cascade trajectories $\xi(\cdot)$ allow a thermodynamical interpretation. The potential $\varphi(\xi_r)$ of Equation 33 given by the drift and diffusion terms, $D^{(1)}(\xi)$ and $D^{(2)}(\xi)$, can be considered the coupling of the trajectory or the subsystem to the bath, whereas the values of ξ_r and its probabilities are the intrinsic features of the individual trajectory. The connection with a possible thermodynamical interpretation becomes clearer if not only the velocity increments are considered but also the transferred energy ϵ_r of the cascade. As shown in Reference 68 (the Langevin equation of the cascade), Equation 17 changes to

$$-r\frac{\partial}{\partial r}\,\xi_r = -\gamma\,\xi_r + m\,\sqrt{\epsilon_r}\,\eta(r),$$
$$-r\frac{\partial}{\partial r}\,\epsilon_r \propto +G\,\epsilon_r + \ldots, \qquad 35.$$

where γ, G, and m are positive values that may depend on r. Note that now the increment process becomes purely additive, a well-known effect (69, 70). Such an in-stationary (r-dependent) Langevin equation can be interpreted in a thermodynamic way, following Reference 67. Interestingly, ϵ_r corresponds to the temperature. As ϵ_r devolves its own fluctuations, the cascades can be considered a mixture of temperatures. Note that after Equation 35, these energy or temperature fluctuations increase in the cascade evolution to smaller scales. In this way the cascade pictures of Kolmogorov (57) and Castaing (19) are set in a new thermodynamic context.

If the complex structure is described correctly by the FPE, the statistics of the entropy values should fulfill the integral fluctuation theorem (IFT),

$$\langle e^{-\Delta S_{\rm tot}}\rangle_N = 1, \qquad 36.$$

a fundamental entropy law of nonequilibrium thermodynamics (cf. 63). Here $\langle\ldots\rangle_N$ denotes the average over many different trajectories for the increments. In **Figure 9**, the distribution of the entropy production values for an experimental data set of a turbulent flow is shown (31). Clearly the mentioned positive and negative entropy values can be seen. The mean value of this distribution $\langle\Delta S_{\rm tot}\rangle$ is positive. By a weighting function $e^{-\Delta S_{\rm tot}}$, negative entropy values contribute much more and must be compensated by many large positive $\Delta S_{\rm tot}$ values so that the IFT Equation 36 is fulfilled. Thus, the IFT is a relation that expresses the balance between the relative frequency of entropy-consuming ($\Delta S_{\rm tot} < 0$) and entropy-producing ($\Delta S_{\rm tot} > 0$) trajectories associated with the stochastic evolution of increment trajectories $\xi(\cdot)$ (individual stochastic trajectories).

In **Figure 9*b***, the obtained values from Equation 36 for increasing numbers of trajectories are shown. The convergence to the absolute value of 1 is well obtained. Already after several thousand values the IFT gets fulfilled.

Another interesting result is obtained for sea waves (60). Extreme events, namely the rogue waves, are characterized by negative entropy values. Comparing different states of the sea waves shows that the statistics $W(\Delta S_{\rm tot})$ change significantly from one state to the other, although for both cases the IFT was fulfilled in high quality. Coming back to the point that the IFT somehow balances the negative and positive entropy events, as the negative entropy events are correlated to large waves, like the rogue waves, we see that this nonequilibrium thermodynamics together with the stochastic cascade process grasps both, i.e., the statistics and the localized structure of the complex disordered system.

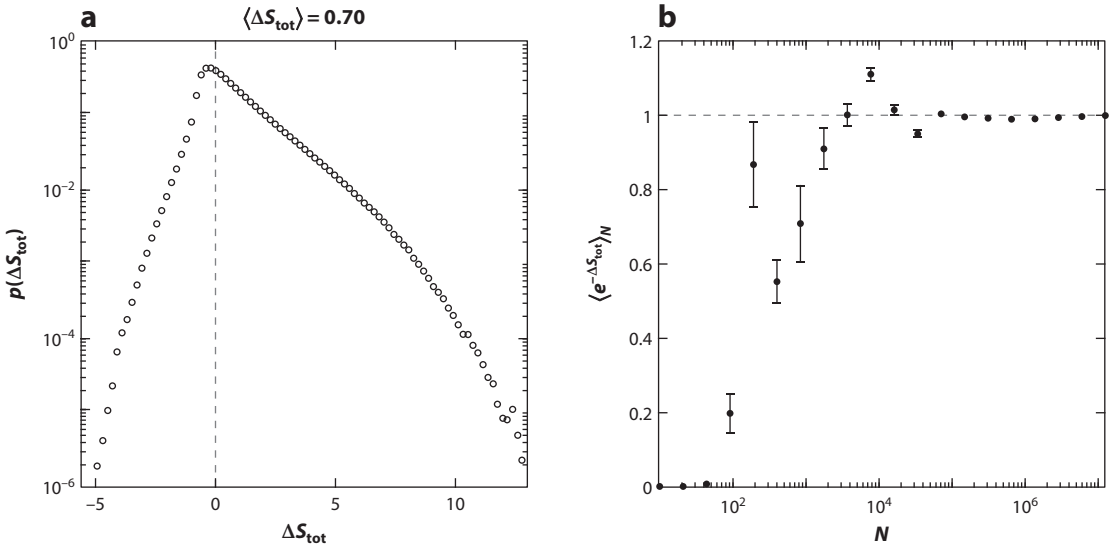

Figure 9

(*a*) Probability density function of the total entropy production ΔS_{tot} obtained from turbulent data, after (71). The mean of the distribution is positive, which means that on average the entropy increases, in accordance with the second law of thermodynamics. For our system here, we find that big fluctuations of the entropy values and pronounced probabilities for negative entropy events exist. Such a distribution is a typical result for data like that shown in **Figure 8**. (*b*) Convergence of the exponential of the entropy production $\langle e^{-\Delta S_{\text{tot}}} \rangle$ for turbulence data, following the IFT in Equation 36. Shown is the evolution of $\langle e^{-\Delta S_{\text{tot}}} \rangle_N$ as a function of the number N of trajectories $\xi(\cdot)$ and its convergence to the value 1. This result shows that the IFT is fulfilled within an accuracy of 1% and better (see Reference 71). Interestingly the IFT implies that the probabilities of the negative and positive entropy events are not arbitrary but balanced by the IFT, which puts much weight on the negative events. In other words, events with negative entropy values must be accompanied by many events with positive entropy to fulfil the IFT law. Abbreviation: IFT, integral fluctuation theorem.

8. CONCLUSIONS

The leading topic of this work was the characterization of complex systems and the question of whether an understanding of the complexity can be achieved by structures as basic elements or if higher-order statistics are needed. For two examples, namely turbulence and sea waves, we showed how these two aspects of structure and statistics are interwoven. The description of the multipoint statistics by a stochastic process of a cascade, or, respectively, by an FPE evolving in scale, allows us to generate surrogate data sets as well as determine entropy values for all data points. For our considered macrosystems, large fluctuations of these entropy values are found, though up till now it has mainly been discussed for microsystems (cf. 63). We see how this concept of microsystems can fruitfully be applied to our considered macrosystems. A key element is the Markov property in scale and the corresponding derivation of the FPE. It is the FPE that leads to a general law of nonequilibrium thermodynamics, namely, the IFT, which is fulfilled for our data with an accuracy of 1% and better. On one hand, the validity of this IFT can be taken as evidence of the consistency of our whole approach. On the other hand, the IFT expresses mathematically the balance between negative and positive entropy values. The exponential weight of the theorem means that each negative entropy value must be compensated by many positive entropy values. This is also true for the structures of the complex systems, as we showed that the negative entropy values relate to the large small-scale structures, which are the challenging properties for turbulence and waves.

Thus, we conclude that our work presents a new consistent approach to the mutuality of order and stochasticity in complex systems.

SUMMARY POINTS

1. N-point statistics representing an all-encompassing probabilistic approach to complex systems can be expressed by $(N-1)$-scale increment statistics. The increment statistics allow a hierarchical ordering. If the increment statistics only depend on increments of the neighboring scale, a three-point closure of the N-point statistics is achieved.
2. The three-point closure of the N-point statistics is equivalent to a stochastic process in scale with Markov property, for which the process equations can be estimated via Kramers–Moyal coefficients from empirical or measured data. If Langevin noise is present, a nonstationary Fokker–Planck equation (FPE) for the cascade process in scale is obtained.
3. The knowledge of the nonstationary scale-dependent FPE allows us to generate numerically new data sets with the same N-point statistics and to forecast single events and also, most interestingly, extreme events.
4. Based on the nonstationary scale-dependent FPE, the entropy production of the cascade trajectory can be defined, for which the rigorous integral fluctuation theorem holds. Thus, a connection with nonequilibrium thermodynamics is given, which balances the occurrence of negative and positive entropy events.

FUTURE ISSUES

1. The nonstationary scale-dependent stochastic description of N-point statistics can be generalized in a straight forward way to higher-dimensional quantities $\vec{q}$, like complex turbulent velocity fields (see Reference 72). Here the FPE depends on different variables of the vector field, and $D^{(1)}$ becomes a vector while $D^{(2)}$ is a diffusion matrix. The problem of how to extend this approach to two- or three-dimensional spaces instead of the one-dimensional cut, for which a hierarchical ordering is evident, remains open.
2. It is a challenge to work out meaningful nonequilibrium thermodynamics of these complex structures, relating it to quantities like energies of the systems. It should also be noted that there have already been different attempts to set up thermodynamical approaches to complex systems. A relation between those would be important.
3. Complex systems are also often described by nonlinear partial differential equations. Is it possible to derive the nonstationary scale-dependent stochastic process equation directly from the partial differential equations? This would unify, at least for these systems, two different means of description.

DISCLOSURE STATEMENT

The authors are not aware of any affiliations, memberships, funding, or financial holdings that might be perceived as affecting the objectivity of this review.

ACKNOWLEDGMENTS

The authors acknowledge funding from the VolkswagenStiftung, the German Science Foundation DFG, and the Ministry for Science and Culture of the State of Lower Saxony (MWK) as well as helpful and inspiring discussions with Bernard Castaing, Christian Behnken, Andreas Engel, Jannik Ehrich, Jan and Rudolf Friedrich, André Fuchs, Mathieu Gibert, Alain Girard, Hauke Hähne, Ali Hadjihossini, Daniel Nickelsen, and Nico Reinke. J.P. acknowledges support from the Laboratoire dexcellence LANEF in Grenoble (ANR-10-LABX-51-01). The authors devote this article to Rudolf Friedrich, with whom we had the pleasure to work out many aspects of this works.

LITERATURE CITED

1. Argyris J, Faust G, Haase M, Friedrich R. 2015. *An Exploration of Dynamical Systems and Chaos*. New York: Springer
2. Heslot F, Castaing B, Libchaber A. 1987. *Phys. Rev. A* 36:5870
3. Haken H. 2004. *Synergetics, Introduction and Advanced Topics*. Heidelberg, New York: Springer
4. Bar-Yam Y. 1997. *Dynamics of Complex Systems*, Vol. 213. Reading, MA: Addison-Wesley
5. Friedrich R, Peinke J, Sahimi M, Tabar MRR. 2011. *Phys. Rep.* 506:87–162
6. Frisch U. 2001. *Turbulence: The Legacy of A. N. Kolmogorov*. Cambridge, UK: Cambridge Univ. Press
7. Davidson PA. 2004. *Turbulence: An Introduction for Scientists and Engineers*. Oxford, UK: Oxford Univ. Press
8. Pope SB. 2000. *Turbulent flows*. Cambridge, UK: Cambridge Univ. Press
9. Clay. 2000. Millennium problems. Clay Mathematics Institute. **http://www.claymath.org/millennium-problems**
10. Nazarenko S, Lukaschuk S. 2016. *Annu. Rev. Condens. Matter Phys.* 7:61–88
11. Onorato M, Residori S, Bortolozzo U, Montina A, Arecchi T. 2013. *Phys. Rep.* 528:47–89
12. Akhmediev N, Ankiewicz A, Taki M. 2009. *Phys. Lett. A* 373:675–78
13. Hussain AF. 1983. *Phys. Fluids* 26:2816–50
14. Kantz H, Schreiber T. 2004. *Nonlinear Time Series Analysis. Cambridge Nonlinear Science Series*. Cambridge, UK: Cambridge Univ. Press
15. Friedrich R, Peinke J. 1997. *Phys. Rev. Lett.* 78:863
16. Peinke J, Friedrich R, Chillà F, Chabaud B, Naert A. 1996. *Z. Phys. B Condens. Matter* 101:157–59
17. Friedrich R, Peinke J. 1997. *Physica D* 102:147
18. Amblard PO, Brossier JM. 1999. *Eur. Phys. J. B-Condens. Matter Complex Syst.* 12:579–82
19. Castaing B, Gagne Y, Hopfinger E. 1990. *Phys. D: Nonlinear Phenom.* 46:177–200
20. Friedrich R, Peinke J, Reza Rahimi Tabar M. 2012. In *Computational Complexity*, ed. R Meyers, pp. 1131–54. New York, NY: Springer
21. Nawroth A, Peinke J. 2006. *Phys. Lett. A* 360:234–37
22. Nawroth AP, Friedrich R, Peinke J. 2010. *New J. Phys.* 12:083021
23. Stresing R, Peinke J. 2010. *New J. Phys.* 12:103046
24. Taylor GI. 1938. *Proc. R. Soc. Lond. A: Math. Phys. Eng. Sci.* 164:476–90
25. Waechter M, Kouzmitchev A, Peinke J. 2004. *Phys. Rev. E*
26. Waechter M, Riess F, Schimmel T, Wendt U, Peinke J. 2004. *Eur. Phys. J. B* 41:259
27. Muzy JF, Bacry E, Arneodo A. 1993. *Phys. Rev. E* 47:875
28. Farge M, Schneider K. 2006. In *Encyclopedia of Mathematical Physics*, ed. JP Françoise, G Naber, TS Tsun, pp. 408–20. Amsterdam: Elsevier
29. Lovejoy S, Schertzer D. 2013. *The Weather and Climate: Emergent Laws and Multifractal Cascades*. Cambridge, UK: Cambridge Univ. Press
30. Friedrich J. 2017. *Closure of the Lundgren-Monin-Novikov hierarchy in turbulence via a Markov property of velocity increments in scale*. PhD Dissertation, Ruhr-Universität Bochum, Germany
31. Renner C, Peinke J, Friedrich R. 2001. *J. Fluid Mech.* 433:383–409
32. Friedrich R, Zeller J, Peinke J. 1998. *Europhys. Lett.* 41:153
33. Tutkun M, Mydlarski L. 2004. *New J. Phys.* 6:49
34. Lück S, Renner C, Peinke J, Friedrich R. 2006. *Phys. Lett. A* 359:335–38

35. Marcq P, Naert A. 2001. *Phys. Fluids* 13:2590–95
36. Hadjihosseini A, Wächter M, Hoffmann NP, Peinke J. 2016. *New J. Phys.* 18:013017
37. Risken H. 1984. *The Fokker-Planck Equation*. Heidelberg: Springer
38. Hänggi P, Thomas H. 1982. *Phys. Rep.* 88:207–319
39. Gardiner CW. 1998. *Handbook of Stochastic Methods for Physics, Chemistry and the Natural Sciences*. Berlin: Springer-Verlag
40. Renner C. 2002. *Markowanalysen stochastisch fluktuierender Zeitserien*. PhD Dissertation, Universität Oldenburg, Germany
41. Renner C, Peinke J, Friedrich R. 2001. *Phys. A: Stat. Mech. Appl.* 298:499–520
42. Einstein A. 1905. *Ann. Phys.* 322:549–60
43. Dubrulle B. 2000. *Eur. Phys. J. B* 14:757–71
44. Kolmogorov AN. 1931. *Math. Ann.* 104:415–58
45. Anvari M, Tabar MRR, Peinke J, Lehnertz K. 2016. *Sci. Rep.* 6:35435
46. Davoudi J, Tabar MRR. 2000. *Phys. Rev. E* 61:6563
47. Friedrich J, Margazoglou G, Biferale L, Grauer R. 2018. *Phys. Rev. E* 98:023104
48. Gottschall J, Peinke J. 2008. *New J. Phys.* 10:083034
49. Honisch C, Friedrich R. 2011. *Phys. Rev. E* 83:066701
50. Siefert M, Kittel A, Friedrich R, Peinke J. 2003. *Europhys. Lett.* 61:466
51. Böttcher F, Peinke J, Kleinhans D, Friedrich R, Lind PG, Haase M. 2006. *Phys. Rev. Lett.* 97:090603
52. Lehle B. 2011. *Phys. Rev. E* 83:021113
53. Lehle B, Peinke J. 2018. *Phys. Rev. E* 97:012113
54. Nawroth AP, Peinke J, Kleinhans D, Friedrich R. 2007. *Phys. Rev. E* 76:056102
55. Castaing B. 1996. *J. Phys. II France* 6:105–14
56. Friedrich R, Peinke J, Naert A. 1997. *Z. Naturforsch* 52a:588–92
57. Kolmogorov AN. 1962. *J. Fluid Mech.* 13:82–85
58. Nickelsen D. 2014. *Markov processes in thermodynamics and turbulence*. PhD Dissertation, Universität Oldenburg, Germany
59. Hallerberg S, Altmann EG, Holstein D, Kantz H. 2007. *Phys. Rev. E* 75:016706
60. Hadjihoseini A, Lind PG, Mori N, Hoffmann NP, Peinke J. 2017. *Europhys. Lett.* 120:30008
61. Laval JP, Dubrulle B, Nazarenko S. 2001. *Phys. Fluids* 13:1995–2012
62. Brown TM. 1982. *J. Phys. A: Math. Gen.* 15:2285
63. Seifert U. 2012. *Rep. Prog. Phys.* 75:126001
64. Nickelsen D, Engel A. 2013. *Phys. Rev. Lett.* 110:214501
65. Reinke N, Nickelsen D, Engel A, Peinke J. 2016. *Progress in Turbulence VI, Proceedings of the iTi Conference on Turbulence 2014, Springer Proceedings in Physics*, Vol. 165, ed. J Peinke, G Kampers, M Oberlack, M Waclawcayk, A Talamelli, pp. 19–25. Heidelberg: Springer
66. Reinke N, Fuchs A, Nickelsen D, Peinke J. 2018. *J. Fluid Mech.* 848:117–53
67. Sekimoto K. 1998. *Prog. Theor. Phys. Suppl.* 130:17–27
68. Renner C, Peinke J, Friedrich R. 2002. arXiv:physics/0211121
69. Gagne Y, Marchand M, Castaing B. 1994. *J. Phys. II* 4:1–8
70. Naert A, Friedrich R, Peinke J. 1997. *Phys. Rev. E* 56:6719–22
71. Fuchs A, Reinke N, Nickelsen D, Peinke J. 2018. In *Proceedings of EUROMECH-ERCOFTAC Colloquium 589: Turbulent Cascades II*, ed. M Gorokhovski. Berlin, New York: Springer. In press
72. Siefert M, Peinke J. 2006. *J. Turbul.* 7:N50